ELSEVIER

Journal of Photochemistry and Photobiology A: Chemistry 125 (1999) 85–91

Journal of Photochemistry and Photobiology A:Chemistry

Effect of transition metals on photoinduced proton transfer from anthrone to 9-anthrol in glasses prepared by the sol–gel method

Tsuneo Fujii[a,*], Nobuaki Tanaka[a], Kazuhiko Kodaira[a], Yoshinobu Kawai[a], Hiromi Yamashita[b], Masakazu Anpo[b]

[a]*Department of Environmental Science and Technology, Faculty of Engineering, Shinshu University, Wakasato, Nagano 380-8553, Japan*
[b]*Department of Applied Chemistry, College of Engineering, Osaka Prefecture University, Sakai, Osaka 593-8531, Japan*

Received 2 December 1998; received in revised form 23 February 1999; accepted 6 April 1999

Abstract

Anthrone has been encapsulated in various xerogels composed of Si and a transition metal from a series of TM=Cr, Fe, Co, Ni, Cu, or Mo by the sol–gel method. EXAFS investigations for typical xerogel samples indicated that the transition metals are highly dispersed in the xerogels. An increase in the fluorescence intensity at 480 nm has been observed under continuous irradiation of the xerogel by 360 nm light. Fluorescence decay curves for typical xerogel samples have also been observed. These results indicate that 9-anthrol is generated efficiently in the xerogels by photoinduced proton transfer. The most effective tautomerization occurred in Si:TM=10000:1 systems and the order for effective metal is Co>Cu>Fe>Mo>Cr≫Ni≅0. It is concluded that an anthrone molecule is coordinated on the transition metal and from which the photochromic behavior occurs by the effective photoinduced proton transfer.

Keywords: Sol–gel reaction; 9-Anthrol; Anthrone; Photochromism; Proton transfer; Transition metal

1. Introduction

Photochemistry of proton transfer processes in excited states is an active field of research [1,2]. Photochromism has great potential for practical applications and for its paramount importance in biological phenomena [1–4]. The photophysical and photochemical processes of aromatic carbonyl molecules in solutions and solid matrixes depend not only on their geometrical and electronic properties of the individual molecules but also the physicochemical properties of surrounding matrixes [5,6].

Nonfluorescent anthrone becomes a fluorescent molecule through keto-enol tautomerization to 9-anthrol [7–12]. In a previous paper [7], we showed that keto-enol photo-isomerization between anthrone and 9-anthrol is responsible for photochromic behavior in the fluorescence spectra of 9-anthrol in Si–Al glasses prepared by the sol–gel method [13–20]. The most effective and remarkable tautomerization occurred in the Si:Al=90:10 system. Thus the characteristic changes observed in the molecule have been substantially explained by the photoinduced proton transfer from the surface Brønsted acid site on the –O–Si–O–Al–O– network to the anthrone molecule encapsulated.

This work reports the influence of some transition metals on the photochromic behavior in the fluorescence spectra of 9-anthrol in xerogel states of 36 systems prepared by the sol–gel method. The systems contain silicon and a transition metal (TM=Cr, Fe, Co, Ni, Cu, or Mo) in different ratios, (Si:TM=100:1, 1000:1, 10000:1, 50000:1, 100000:1, and 1000000:1) and a small amount of HCl as a catalyst at a constant temperature (300 K). The fluorescence lifetimes and EXAFS spectra in typical xerogels have been also measured. It was found that anthrone molecules encapsulated into the xerogels interact with the transition metal. This interaction is responsible for the photochromic behavior in the fluorescence spectra originated from the photoinduced proton transfer.

2. Experimental details

Anthrone (Wako JIS 1st grade) was purified by repeated recrystallization from acetic acid and an ethanol–water mixture. Ethanol, acetic acid, HCl, $CrCl_3$, $FeCl_3$, $CoCl_3$, $NiCl_2$, $FeCl_3$, and $MoCl_2$ supplied by Wako (S.S.G., JIS S, or JIS reagent grade), TEOS (tetraethyl orthosilicate) from

*Corresponding author. Tel.: +81-26-2695535; fax: +81-26-2695550; e-mail: tsfujii@gipwc.shinshu-u.ac.jp

1010-6030/99/$ – see front matter
PII: S1010-6030(99)00093-3

Shin-Etsu Chemicals were used without further purification. Water was deionized and distilled.

A 5×10^{-4} M (M=mol dm^{-3}) solution of anthrone (9-anthrol) in ethanol was prepared. The starting solutions of the reaction systems contained 10.0 cm^3 of the anthrone solution, 10 cm^3 mixtures of TEOS, ethanol solution of the transition metal chloride, and 0.2 cm^3 of a 1.0×10^{-4} M HCl in aqueous solution. The solutions were stirred during the gradual addition, and stirred thoroughly for a further 10 min and the total volumes were adjusted to 20.2 cm^3 in the vial. In order to observe continuous fluorescence and excitation spectra, a 3 cm^3 aliquot of the mixed solutions were poured into individual plastic cells. The procedures were all carried out under a nitrogen atmosphere. The molar ratios of Si:TM (Cr, Fe, Co, Ni, Cu, and Mo) were 100:1, 1000:1, 10000:1, 50000:1, 100000:1, and 1000000:1 for the systems, abbreviated as systems Co-2, Co-3,. . ., and Co-6,. . ., Cu-6,. . ., and Mo-6, etc., respectively. The ratio of 9-anthrol (anthrone) to the transition metal is 1:1 for the 10000:1 sample.

The cells were covered with a thin film with three pin holes and allowed to undergo a sol–gel–xerogel reaction at 300 K under dark conditions. The emission spectra were observed using a Shimadzu RF-5000 fluorescence spectrometer by the surface-emission method at room temperature. In the photochromic experiments the gels were set for more than 100 days after preparing the starting solution. The relative fluorescence intensity at the starting point of the photochromic observation was adjusted using the fluorescence intensity of anthracene in cyclohexane (1.0×10^{-4} M). The time variation of the fluorescence intensity at 480 nm with continuous irradiation of light at 360 nm was observed every 10 or 20 s. The data were transferred to an NEC PC-9801 personal computer for processing.

The procedures for the fluorescence decay measurements are the same as the previous paper [7]. The TM-2, TM-3, and TM-4 (TM=Co, Cu, and Mo) xerogel systems over one year were measured. The fluorescence decay curves of 9-anthrol encapsulated in the xerogels cannot be represented by a single exponential and can be well described by

$$I(t) = A_1 \exp(-t/\tau_1) + A_2 \exp(-t/\tau_2). \quad (1)$$

The average lifetime, $\bar{\tau}$, relative fluorescence quantum yields, φ_1^r and φ_2^r, were calculated as previously [7,21]. Surface-emission method was performed for the fluorescence, excitation, and fluorescence decay measurements. The EXAFS (extended X-ray absorption fine structure) for Co-2 and Cu-2 samples over one year were measured in the fluorescence mode at 295 K by a Rigaku R-EXAFS 2000F Laboratory EXAFS Spectrometer. The normalized spectra were obtained by a procedure described in previous literature [22] and Fourier transformation (uncorrected for phase shift) was performed on k^3-weighted EXAFS oscillations in the range of 3–12 Å^{-1}. The curve-fitting of the EXAFS data was carried out by employing the iterative nonlinear least-squares method of Levernberg [23] and the empirical back scattering parameter sets extracted from the shell features of copper compounds.

3. Results and discussion

3.1. Fluorescence spectra during the sol–gel–xerogel transitions

The fluorescence spectra of 9-anthrol during the sol–gel–xerogel transitions of the reaction systems are characterized by the Si-to-TM ratio of the reaction systems. Four fluorescent bands of 9-anthrol in Si–Al gels were classified [7]. They are the hydrogen-bonded neutral ($\lambda_{F,max}\cong455$ nm) observed in ethanol, etc., the complex ($\lambda_{F,max}\cong480$ nm) observed in alcohol solutions of metal alkoxide such as diisobutoxyaluminum triethylsilane[$(OBu^i)_2$–Al–O–Si–$(OEt)_3$] and gel, the ion-pair ($\lambda_{F,max}\cong540$ nm) observed in solution of tetraethyl amine and gel and the anion ($\lambda_{F,max}\cong560$ nm) observed in basic solutions and gel. Relatively strong interaction between 9-anthrol and metal may be responsible for the complex formation.

Fig. 1 shows the typical fluorescence spectra of 9-anthrol during the sol–gel–xerogel transitions of the sample Co-4 as a function of time. Just after mixing the solution and at 5 days, the spectra showed a peak at 454 nm corresponding to the hydrogen-bonded neutral species. The spectrum observed at 12 days showed a broad peak at 480 nm which is assigned to the complex species. In addition to the above two fluorescent species, the spectrum observed at 145 days has some contribution at around 550 nm. This contribution is due to the ion-pair at around 540 nm and/or the anion at around 560 nm. These peak positions are red-shifted compared with those observed in solutions [8].

Although the excitation wavelength dependence of the fluorescence spectra of 9-anthrol at 145 days for the sample Co-4 are not shown here, it showed that the fluorescence spectra show only a peak at 480 nm except for excitation at 470 nm. The fluorescence spectrum excited at 470 nm shows a shoulder around 560 nm. However, there is apparent

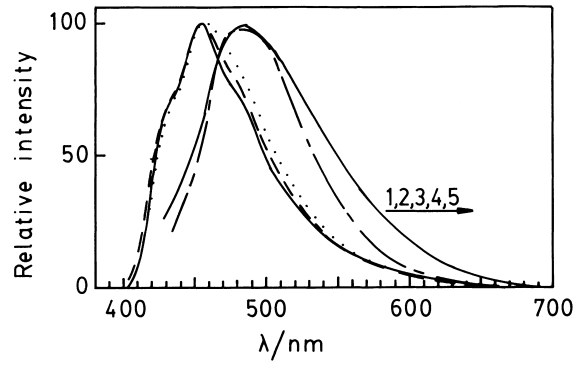

Fig. 1. Fluorescence spectra of 9-anthrol excited at 368 nm during the sol–gel–xerogel transition for sample Co-4: (1) just after the mixing, (2) 5 days, gelation was observed, (3) 12 days, (4) 41 days, and (5) 145 days.

excitation-wavelength dependence in the fluorescence spectra of 9-anthrol for samples Si–Al systems [7]. This is a marked difference between the fluorescence spectra observed in Si–Al systems and Si–TM systems. The difference is attributable to the different presence of metal concentration where Al/(Si+Al)=0.01 to 0.99 and Si–TM systems where TM/(Si+TM)=0.000001 to 0.01. In the Si–TM systems, it can be interpreted that 9-anthrol exist relatively in homogeneous environment than Si–Al systems. Although contribution of the four fluorescent bands to the spectrum of the individual sol–gel reaction systems depends on the Si-to-TM ratio, the observed excitation wavelength dependence of the fluorescence spectra are composed of the four fluorescent bands and the main component around 480 nm is hydrogen-bonded and complex species. The contribution from ion-pair and anionic species is very small.

3.2. EXAFS and FT-EXAFS spectra

Fig. 2 shows the EXAFS and FT-EXAFS spectra of the Cu-2 and Co-2 samples. EXAFS spectrum for Cu-2 sample (2a) shows strong and sharp band. As shown in Fig. 2(a'), the Cu-2 sample exhibits a strong peak at around 1.6 Å and fitting parameter for coordination number is 2.8. These values correspond to the reported Cu^{+}/Y-zeolite [23]. The value 1.6 Å can be assigned to the neighboring O-atoms (Cu–O) of the –O–Si–O–Cu–O– network indicating the presence of a planar 2- or 3-coordinate isolated Cu^{+} ions. The spectra for the system Co-2 shown in Fig. 2(b) and (b') show a very strong peak at around 1.5 Å and fitting parameter for coordination number is 3.4. These values indicate that the presence of 4-coordinate isolated Co^{2+} ions in the –O–Si–O–Co–O– network. These results describe that there are no aggregations of the Cu^{2+} and Co^{2+} ions in the prepared gels. This conclusion can safely be applied to the other samples for Cr, Fe, Co, Ni, Cu and Mo systems and the transition metals are distributed homogeneously in the Si–TM samples prepared.

3.3. Fluorescence lifetimes of 9-anthrol encapsulated in Si–TM binary oxide xerogels

The changes in the fluorescence lifetime of mixed luminescent compounds reflect environment changes in heterogeneous systems. Typical fluorescence decay curves of 9-anthrol encapsulated in Co-2 and Co-3 xerogels are shown in Fig. 3. The monitored wavelength was 480 nm. In Section 3.1, it is shown that the contribution from the fluorescences originated from the hydrogen-bonded neutral and the complex species are the main species in 480 nm emission [7]. The deconvolution was performed by assuming a double-exponential decay as Eq. (1) and the results are indicative of a good fit. The data determined by this method, the short and long fluorescence lifetimes (τ_1 and τ_2) the coefficients (A_1 and A_2), the average lifetime, $\bar{\tau}$, and relative fluorescence quantum yield, φ_1^r, the relative fluorescence

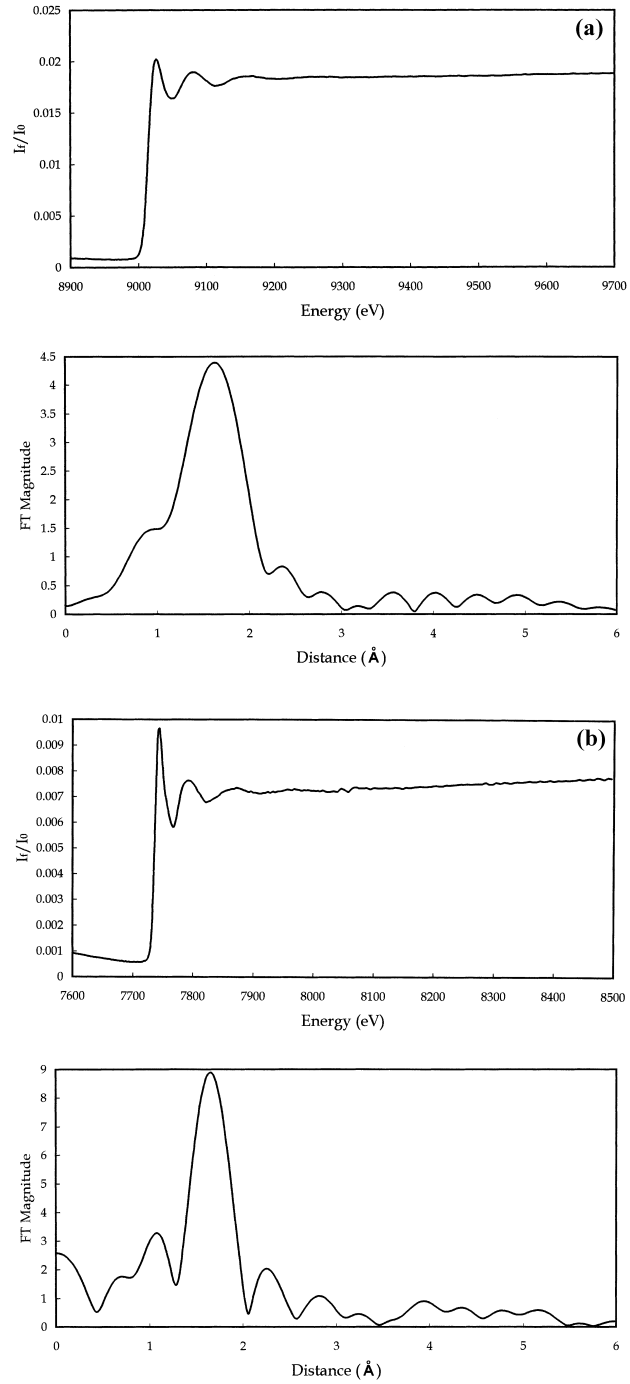

Fig. 2. EXAFS ((a) and (b)) and FT-EXAFS ((a′) and (b′)) spectra of the Cu-2 and Co-2 gels.

quantum yield from the hydrogen-bonded species, and φ_2^r, the relative fluorescence quantum yield from the complex species, are given in Table 1, also including the data for the pure Si system. The short and long fluorescence lifetimes (τ_1 and τ_2) to the hydrogen-bonded and complex fluorescences [7], respectively. The τ_1 and τ_2 in the present systems are ca. 1–4 ns and 8–14 ns, respectively. These values are shorter than for those observed in pure Si and Si–Al systems indicating an enhancement of the interaction between 9-

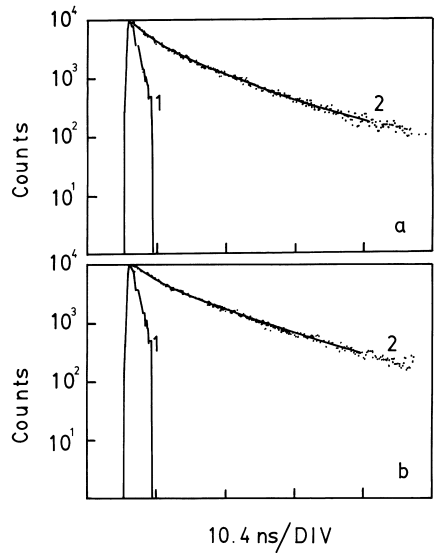

Fig. 3. Fluorescence decay curves of 9-anthrol encapsulated in samples Co-2 (a) and Co-4 (b): (1) excitation pulse profile; (2) decay curve monitored at 480 nm.

anthrol and the surrounding matrix in the Si–TM gels. $\bar{\tau}$ is in the order of Si–Co>Si–Mo>Si–Cu, indicating radiationless rate in the Si–TM systems, especially in the Si–Cu systems, becomes faster than those in the pure Si and Si–Al systems. φ_2^r is dominant in all systems containing transition metal and the values are ca. 0.7–0.9. This indicates that coordination of anthrone to the transition metals is to be preferential case in the gels including transition metal.

3.4. Influence of transition metals on the photochromic behavior in the fluorescence spectra of 9-anthrol encapsulated in the gels

In the previous paper, we found that continuous light irradiation at 360 nm on the Si–Al gel systems including anthrone and/or 9-anthrol changes the fluorescence intensity around 480 nm (mainly composed of the contribution from the hydrogen-bonded neutral and the complex fluorescences). It is important to examine the change in the fluorescence intensity for the gel samples containing transition metals under the same conditions. The excitation wavelengths, 368 and 400 nm were examined for the photochromic behavior in the fluorescence spectra. The former light is absorbed by the anthrone molecule and the latter is not. The photochromic behavior occurred only by 368 nm excitation. These results indicate that photoabsorption of anthrone in the gel samples is essential for the photochromic behavior in the fluorescence spectra of 9-anthrol.

Two typical results for the relative intensity changes at 480 nm for the Si–TM (TM=Co and Cu) systems, $I_{(480\ nm)}$ vs. the irradiation time are shown in Fig. 4. It is noted that induction period for photochromic behavior appeared more or less for all systems [24–26], though reaction mechanism is not clear at the present time. Just after the start of irradiation, the fluorescence intensity increases rapidly as a function of time. This increase is due to occurrence of the photoinduced proton transfer from anthrone to 9-anthrol in the gels. On the other hand, after peaking the maximum, the formation of the anionic species and/or nonfluorescent species would be responsible for the decrease in the fluorescence intensity at ca. 480 nm. Similar photochromic behavior in the fluorescence intensity was observed for the Si–TM (TM=Cr, Fe, and Mo) systems. The photochromic behavior, however, was scarcely observed for the Si–Ni systems. This may be due to the efficient photoabsorption by the Ni ions in the gels.

First-order plots during the initial period of irradiation for the systems Si–TM (TM=Co and Cu) are shown in Fig. 5. Clear linear relationships were obtained for the systems indicating that a first-order photoinduced proton transfer reaction occurs in these systems. These results suggest that

Table 1
The fluorescence lifetimes (τ_1 and τ_2), their coefficients (A_1 and A_2), average lifetime ($\bar{\tau}$) and relative fluorescence quantum yields (φ_1^r and φ_2^r) of 9-anthrol in various gels

	τ_1 (ns)	τ_2 (ns)	A_1	A_2	$\bar{\tau}$ (ns)	φ_1^r	φ_2^r
Si:Co							
100:1	2.6	10.5	0.032	0.031	8.9	0.20	0.80
1000:1	1.5	10.3	0.046	0.049	9.2	0.12	0.88
10000:1	3.6	14.3	0.024	0.040	12.8	0.13	0.87
Si:Cu							
100:1	0.97	7.8	0.086	0.025	5.8	0.30	0.70
1000:1	1.7	11.2	0.064	0.025	8.5	0.28	0.72
10000:1	4.2	12.8	0.031	0.041	10.2	0.21	0.79
Si:Mo							
100:1	1.2	10.5	0.080	0.026	8.1	0.26	0.74
1000:1	1.1	10.3	0.077	0.031	8.4	0.20	0.79
10000:1	3.4	11.9	0.018	0.061	11.2	0.08	0.92
Pure Si[a]	7.0	16.7	0.023	0.005	10.3	0.66	0.34

Excitation wavelength: 337 nm, monitored at 480 nm, at 295 K.
[a] Taken from Ref. [7].

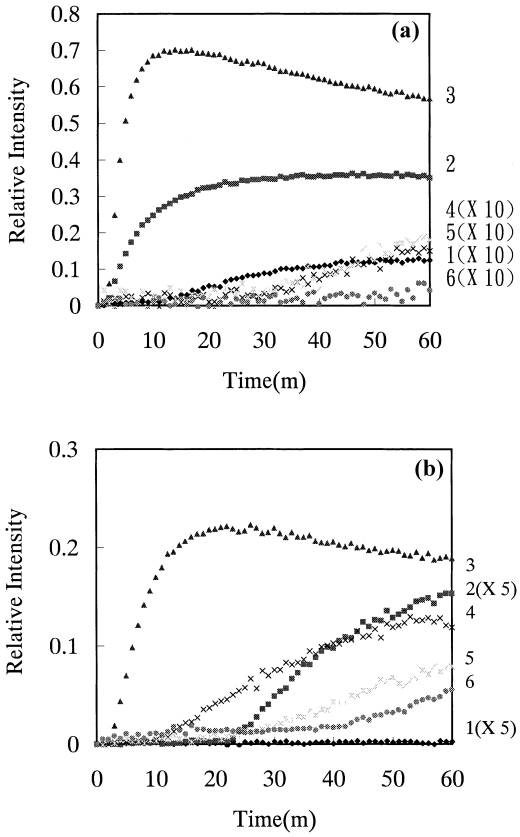

Fig. 4. Change in the fluorescence intensity of 9-anthrol at 480 nm by 360 nm excitation: (a) 1–6: Co-2, Co-3, Co-4, Co-4.5, Co-5, and Co-6; and (b) 1–6: Cu-2, Cu-3, Cu-4, Cu-4.5, Cu-5, and Cu-6.

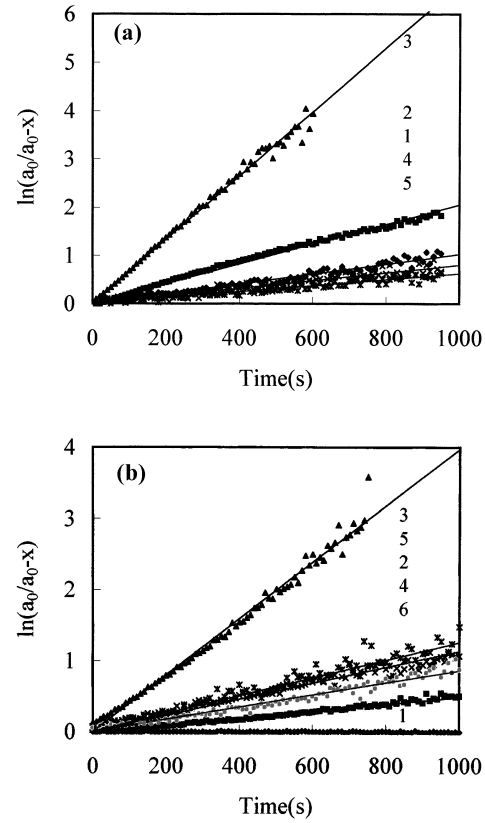

Fig. 5. First-order plot of $\ln[a_0/(a_0-x)]$ vs. time: (a) 1–6: Co-2, Co-3, Co-4, Co-4.5, Co-5, and Co-6; and (b) 1–6: Cu-2, Cu-3, Cu-4, Cu-4.5, Cu-5, and Cu-6.

the rise in time is directly proportional to the residual concentration of anthrone. Fig. 6 plots the obtained first-order reaction constant, k, and I_{max}/I_0 vs. TM/Si for the systems. The order of k was found to be Si–Co>Si–Cu>Si–Fe>Si–Mo>Si–Cr≫Si–Al≫Si–Ni≅0 and TM-4>TM-3>TM-4.5>TM-5≈TM-6≈TM-2. These order for the Si–TM systems are two order larger than those for the Si–Al systems. It is noted that the order is TM-4>TM-3>TM-2. The results indicate that various interaction between one 9-anthrol and transition metals in the ground state and/or energy transfer from excited 9-anthrol to surrounding transition metals may be responsible for effective deactivation processes in TM-3 and TM-2.

3.5. Influence of transition metals on the change in chemical species during light irradiation

It is interesting to compare the fluorescence spectra of 9-anthrol in the gels just before and after the light irradiation. Fig. 7 shows the fluorescence and excitation spectra of 9-anthrol in Co-4, Cu-4 and Fe-4 systems. In the Co-4 system, the fluorescence spectrum before light irradiation is weak and it's peak is located at 480 nm. The corresponding excitation spectrum showed a peak at 395 nm. After the irradiation, the fluorescence intensity became strong. The peak wavelengths for fluorescence and excitation spectra are at 476 and 375 nm, respectively. These results indicate that the contribution from the ion pair and/or anion species is small compared with the contribution from the complex species. The amount of the complex species is enhanced by light irradiation and the contribution from the complex species at around 480 nm becomes the major fluorescent species.

In the case of Fe-4, the fluorescence and excitation peaks are located at 470 and 385 nm, respectively, and the change in the fluorescent intensity during the sol–gel reaction is not as large compared with the systems of Co. The fluorescence peaks before and after the irradiation are located at the same wavelength 486 nm. The peak wavelength for the excitation spectra before and after irradiation are located at the same wavelength 397 nm. This unchanged behavior indicates that the main ground-state species before and after the irradiation in the Fe-4 system is the complex. This behavior suggests that proton transfer is relatively effective in this system, though there may be radiationless processes in the system.

In the case of Cu-4, the fluorescence peaks observed before and after irradiation are located at around 470 and 487 nm, respectively. The excitation spectrum before the irradiation has a peak at 375 nm. The spectral peak after the irradiation is broad and its peak wavelength is located

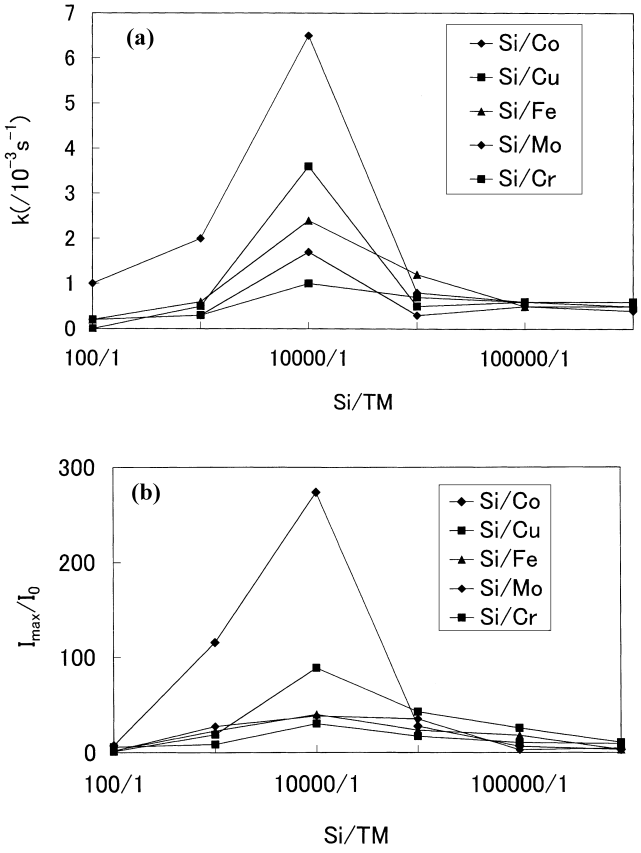

Fig. 6. Relations between (a) k vs. TM/Si; and (b) I_{max}/I_0 vs. TM/Si for the systems.

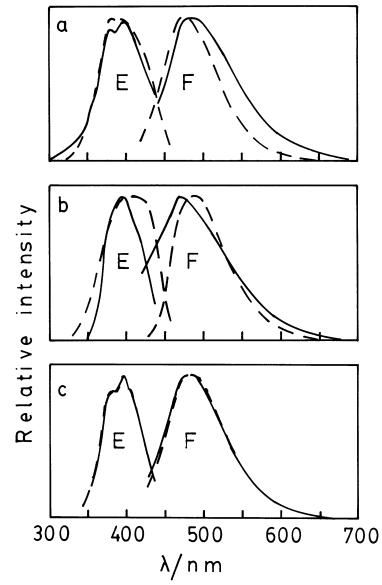

Fig. 7. Change in the fluorescence and excitation spectral feature before and after light irradiation at 368 nm for Co-4 (a), Cu-4(b), and Fe-4 (c) systems.

around 400–420 nm. This change indicates that the ground-state species before and after the irradiation in Cu-4 system are the complex and the ion-pair, respectively. The changes in the fluorescence intensity is relatively large among the gels studied. These behavior suggest that the proton transfer is effective in this system, though intensity change in the fluorescence spectra is small compared with the case of Co. The small change in spectral shape suggests that there may be energy transfer from the excited complexes to surrounding matrix and/or Cu. A similar spectral situation was observed for the Mo-4 systems, though fluorescence intensity after the light irradiation is weaker than the case of Cu. This indicates that the complex formation before the irradiation in the Mo-4 system is enough and the intensity change before and after the irradiation in the Mo-4 systems is small compared with the systems for the Co and Cu systems. In the case of Cr-4, though less spectral changes were observed, the overall spectral feature before and after the light irradiation were similar to the case of Mo.

3.6. Photoinduced proton transfer mechanism in the gels containing transition metal

In Si/Al systems, the most effective and remarkable tautomerization occurred in the Si:Al=90:10 system, and it was concluded that the photochromic behavior occurs by the photoinduced proton transfer from the Brønsted acid sites on the –O–Si–O–Al–O– network to the anthrone molecules. The results shown in Fig. 6, however, indicate that the most effective systems are the Si:TM=10000:1 systems in which the ratio of anthrone to transition metal is 1:1. The analysis of the fluorescence lifetimes for the prepared gels indicates that the complex formation (coordination of 9-anthrol to the transition metals) is the preferential case in the gels including the transition metals. This result and spectral changes during the light irradiation indicate that the complex formation between anthrone and transition metal in the xerogels is responsible for the photoinduced proton transfer. The following scheme illustrates the photoinduced proton transfer from anthrone (An) to 9-anthrol (9-AnOH) including the transition metal (TM) in the prepared gel matrixes.

$$\mathrm{An{-}TM} \xrightarrow[\text{Photoinduced proton transfer}]{h\nu} \mathrm{9\text{-}AnOH{-}TM}$$

In conclusion, the efficiency of the photoinduced proton transfer in the prepared gel matrix including the transition metals is much more enhanced compared with those of the systems including no transition metals and in Si–Al systems. This enhancement is due to the coordination of anthrone on the transition metal in the prepared gels.

Acknowledgements

The authors thank RIGAKU CORP. for the EXAFS measurements. This work was supported in part by the Grant-in-Aid on Priority-Area-Research "Photoreaction

Dynamics'' from the Ministry of Education, Science, Sports and Culture of Japan (No. 08218225).

References

[1] A. Gilbert (Ed.), Photochemistry, vol. 27, The Royal Society of Chemistry, Cambridge, 1996.
[2] V. Ramamurthy (Ed.), Photochemistry in Organized and Constrained Media, VCH, New York, 1991.
[3] H. Dürr, H. Bouas-Laurent (Eds.), Photochromism. Molecules and Systems, Elsevier, Amsterdam, 1990.
[4] M. Anpo, T. Matsuura (Eds.), Photochemistry on Solid Surfaces, Elsevier, Amsterdam, 1989.
[5] J.B. Birks, Photophysics of Aromatic Molecules, Wiley/Interscience, London, 1970.
[6] N. Mataga, R. Kubota, Molecular Interactions and Electronic Spectra, Marcel Dekker, New York, 1970.
[7] T. Fujii, K. Kodaira, O. Kawauchi, N. Tanaka, H. Yamashita, M. Anpo, J. Phys. Chem. B 101 (1997) 10631.
[8] T. Fujii, S. Mishima, N. Tanaka, O. Kawauchi, K. Kodaira, H. Nishikiori, Y. Kawai, Res. Chem. Intermed. 23 (1997) 829.
[9] Y. Bansho, K. Nukada, Bull. Chem. Soc. Jpn. 33 (1960) 579.
[10] H. Baba, T. Takemura, Bull. Chem. Soc. Jpn. 37 (1964) 1241.
[11] H. Baba, T. Takemura, Tetrahedron 24 (1968) 4779.
[12] T. Takemura, H. Baba, Tetrahedron 24 (1968) 5311.
[13] D. Avnir, V. Kaufman, R. Reisfeld, J. Phys. Chem. 88 (1984) 5956.
[14] S. Sakka, Zoru-geru-houno no kagaku (Science of the Sol–Gel Method), Agne Shofu Sha, Tokyo, 1988.
[15] C.J. Brinker, G.W. Scherer, Sol–Gel Science: The Physics and Chemistry of Sol–Gel Processing, Academic Press, New York, 1990.
[16] B. Dunn, J.I. Zink, J. Mater. Chem. 1 (1991) 903.
[17] J.I. Zink, B.J. Dunn, Ceram. Soc. Jpn. 99 (1991) 878.
[18] D. Avnir, S. Braun, M. Ottolenghi, Am. Chem. Soc. Symp. Ser. 499 (1992) 384.
[19] D. Avnir, Acc. Chem. Res. 28 (1995) 328.
[20] T. Fujii, Trend Photochem. Photobiol. 4 (1994) 243.
[21] R.K. Bauer, R. Borenstein, P. de Mayo, K. Okada, M. Rafalska, W.R. Ware, K.C. Wu, J. Am. Chem. Soc. 104 (1982) 4635.
[22] K. Omote, K. Tohji, Y. Waseda, A. Kiku, M. Funahashi, J. Appl. Phys. 21 (32-2) (1993) 267.
[23] H. Yamashita, M. Matsuoka, K. Tsuji, Y. Shioya, M. Anpo, M. Che, J. Phys. Chem. 100 (1996) 397.
[24] M.A. Fox, M.T. Dulay, Chem. Rev. 93 (1993) 341.
[25] Y. Sakata, T. Yamamoto, H. Gunji, H. Imamura, S. Tsuchiya, Chem. Lett. (1998) 131.
[26] Y. Sakata, T. Yamamoto, T. Okazaki, H. Imamura, S. Tsuchiya, Chem. Lett. (1998) 1253.